

Effects of Aging and Biological Sex on the Acoustical Properties of Murine Skulls

Wendy Zimmerman, Alec Batts¹ & Elisa Konofagou^{1,2,1}
Department of Biomedical Engineering, ²Department of Radiology
Columbia University, New York, NY

Acknowledgements

National Institutes of Health

- R01AG038961
- R01EB009041

Focused Ultrasound Foundation

Columbia University and Amazon Summer

Undergraduate Research Experience (SURE) Program

UEIL Lab Members:

- Sua Bae (PhD)



wz2623@columbia.edu

Introduction & Objectives

Focused Ultrasound (FUS)-mediated Blood Brain Barrier (BBB) Opening Technique

- FUS is a noninvasive treatment for a broad range of clinical conditions via tissue destruction or targeted drug therapy ^[1]
- For targeted drug therapy, it can be used to induce steady oscillations of systemically administered microbubbles, which induces moderate and reversible changes in vasculature ^[1]
- This technique can be employed to open the BBB, a part of the NVU created by the tight junctions between endothelial cells that results in a barrier which prevents 98% of small molecule drugs from passing into the brain, allowing therapeutic drugs that treat diseases such as Parkinson's and Alzheimer's to enter the brain ^{[1], [2], [3]}

Attenuation Caused by the Skull

- FUS beams are distorted by skulls due to their structure and composition leading to a need to understand precisely how the beams are affected to achieve the most accurate results possible ^[2]
- Those properties are affected by both age, which is characterized by an overall increase in skull thickness and trabecular bone porosity ^{[4], [5], [6]}, and biological sex, which is characterized by biological females having a higher degree and faster rate of bone loss, resulting in a greater porosity ^{[4], [6]}

Objectives

- 1) **Determine the effect of age, biological sex, and strain on acoustic insertion loss through the parietal and frontal murine skull regions**
- 2) **Perform a bilateral sonication on a mouse using FUS with an experimentally determined correction factor for insertion loss and determine the BBB opening volumes using contrast-enhanced MRI**

[1] Batts et al., *IEEE Trans. Biomed. Eng.*, 2022

[4] Junbo Shim et al., *Sci. Rep.*, 2022

[2] Ko-Ting Chen et al., *Front. Pharmacol.*, 2019

[5] Elizabeth M. Lillie et al., *ASBMR*, 2015

[3] Kelsie F. Timbie et al., *JCR*, 2015

[6] Huayue Chen, *Int. J. Endocrinol.*, 2013

Materials & Methods

Experimental Calculation of Insertion Loss Through Murine Skull

- Excised skulls were placed in 6-well plates with deionized water and degassed 24 and 3 hours prior to beginning the attenuation experiments
- A 1.5 MHz FUS transducer and custom-made, 3D printed water bath were filled with degassed water and placed into the attenuation measurement setup (Figure 1)
- A 300 mV voltage was applied to the FUS transducer and raster scans in the axial and circumferential dimensions (Figure 2) were performed (without the plate on the shelves) to focus the needle hydrophone at the center of the acoustic focus
- The plate was placed on the shelves and a free field average peak negative pressure (PNP) measurement was taken using the PicoScope
- The insertion loss in the left parietal, left frontal, right frontal, and right parietal murine regions (Figure 3) was measured using the hydrophone and calculated using the equation to the right for a total of 27 degassed skulls (Table 1)

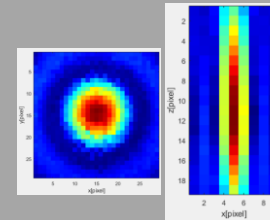


Figure 2: Example of raster scans in the axial (left) and circumferential (right) dimensions

Age Groups			Biological Sex		Strain				
Young (0-6 months)	Middle-Aged (7 month-1.7 years)	Old Aged (1.8-2.3 years)	Female	Male	C57BL/6J (wild type)	balb/c	Tta	Tau	3xTg
7	11	9	14	13	15	3	2	3	5

Table 1: Sample sizes for skull insertion loss measurements

$$Insertion Loss = \frac{Regional Pressure}{Free Field Pressure} * 100$$

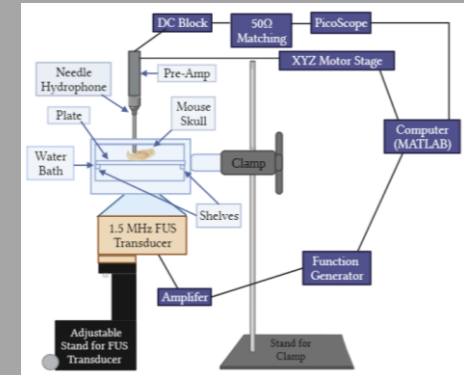


Figure 1: Attenuation measurement setup

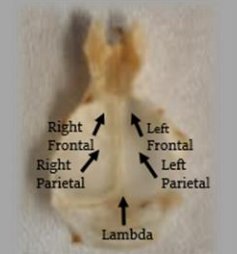


Figure 3: Murine skull regions insertion loss was measured through, chosen as they are popular targets for Alzheimer's and Parkinson's disease research

- The process was performed on one of the skulls twice, when it was not degassed and when it was to demonstrate the effect of degassing the skulls (Figure 4)

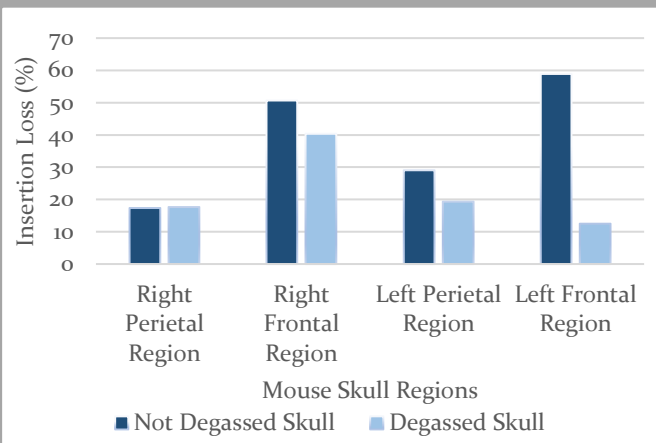


Figure 4: A comparison between a non-degassed and degassed skull showing that degassing reduces the attenuation through the skull

In vivo FUS-mediated BBB opening using experimentally-determined insertion loss correction factor

- Using the 1.5 MHz FUS transducer, BBB opening procedures were performed separately on the right and left hippocampi (with 20 minutes in between to allow the initial bolus of microbubbles to leave the circulatory system) of a 9 week old, C57BL/6J (wild type) mouse at PNP of 450 kPa with a PRF 10 Hz and a pulse length of 10000 cycles using a correction factor for experimentally-determined insertion loss of 20%
- A contrast-enhanced MRI in the axial and coronal orientations was performed on the mouse and used to calculate the BBB opening volume

Results

Acoustic Insertion Loss: The Effect of Biological Properties on Acoustic Transmission Through Skull

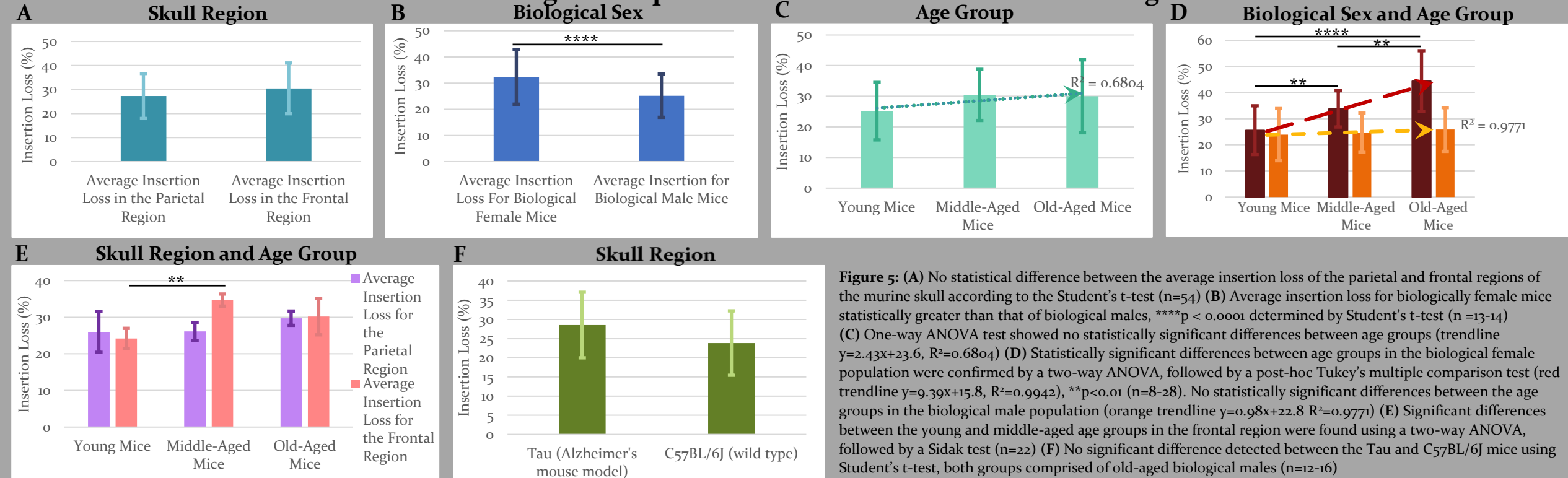
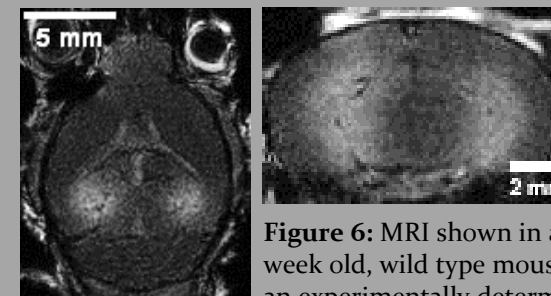


Figure 5: (A) No statistical difference between the average insertion loss of the parietal and frontal regions of the murine skull according to the Student's t-test ($n=54$) (B) Average insertion loss for biologically female mice statistically greater than that of biological males, $****p < 0.0001$ determined by Student's t-test ($n=13-14$) (C) One-way ANOVA test showed no statistically significant differences between age groups (trendline $y=2.43x+23.6$, $R^2=0.6804$) (D) Statistically significant differences between age groups in the biological female population were confirmed by a two-way ANOVA, followed by a post-hoc Tukey's multiple comparison test (red trendline $y=9.39x+15.8$, $R^2=0.9942$), $**p < 0.01$ ($n=8-28$). No statistically significant differences between the age groups in the biological male population (orange trendline $y=0.98x+22.8$, $R^2=0.9771$) (E) Significant differences between the young and middle-aged age groups in the frontal region were found using a two-way ANOVA, followed by a Sidak test ($n=22$) (F) No significant difference detected between the Tau and C57BL/6J mice using Student's t-test, both groups comprised of old-aged biological males ($n=12-16$)

- No statistically significant difference between frontal and parietal murine skull regions
- Average insertion loss significantly greater in biologically female mice
- Average insertion loss through the murine skull generally increases with age, significantly for biologically female mice
 - Increase in average insertion loss for biological female mice could be driving force behind results seen in Fig.5C
- No statistically significant difference was shown for the average insertion loss for Tau and C57BL/6J mice, isolated from age and biological sex variables
 - Alzheimer's models tend to have osteoporosis leading them to have slightly thicker skulls than wild type mice, which, although not significant, can be seen in Fig.5F

In Vivo BBB Opening: BBB Opening Depicted Using a Contrast-Enhanced MRI



- BBB opening volumes for the right and left hemisphere were 22.196 mm^3 and 23.472 mm^3 respectively (Figure 6)

Figure 6: MRI shown in axial (left) and coronal (right) orientations of a 9 week old, wild type mouse that underwent a BBB opening procedure using an experimentally determined correction factor

Discussion & Conclusions

Possible Explanations of Results

- **No statistical difference between the frontal and parietal regions of the murine skull**
 - A greater skull thickness is associated with a greater insertion loss in murine models [7] and the frontal region of murine skull is thicker than parietal region
 - Incidence angle and reflections could have resulted in a lower average incidence for the frontal region than expected due the curvature and size of the skull and placement on the plate [8]
- **General increase in average insertion loss with age**
 - In both biological sexes, a general increase in skull thickness has been observed with an increase in age [4], [5], [6]
 - After reaching final development state a plateau of thickness occurs [9], which can be observed in Fig.5.C
 - Overall, as mice age, a greater porosity of trabecular bone and cortical bone density has been observed which contribute both to skull thickness and insertion loss [4]
- **Statistical difference in average insertion loss in biologically male and female mice**
 - A greater increase in trabecular separation and decrease in trabecular bone volume fraction and in trabecular bone density in has been observed in biologically female mice when compared to their male counterparts [4]
 - This is likely due to biologically female mice having a higher degree and faster rate of bone loss, resulting in a greater porosity of trabecular bone [4],[5],[6]
 - Decrease in estrogen levels increases osteoclast (a bone degrading cell) formation and survival leading to greater bone resorption [10] potentially explaining the phenomena seen in Fig.5.D

Limitations

- Skulls are very heterogeneous structures, varying extensively between subjects, making it difficult to establish overall trends (Figure 7)
- Both incidence angle, which can significantly affect attenuation measurements as it becomes less orthogonal [8], [9], and body mass, which can affect the size of the skull and has been correlated to skull thickness and insertion loss [7], were not accounted for in this study
- The excision process resulted in, overall, varied skull shapes and required the removal of the bottom of the skull, which can cause attenuation and distortion effects (e.g. standing waves), although at the low frequency used those effects are not predicted to have a significant effect [11]
- Skulls were from a limited number of ages and strains

Future Work

- Micro-CT analysis to quantify the changes in the microstructure of skulls, specifically the skull thickness and porosity
- Effect of estrogen on skull structure and insertion loss
- Enhance distribution of ages and strains of samples

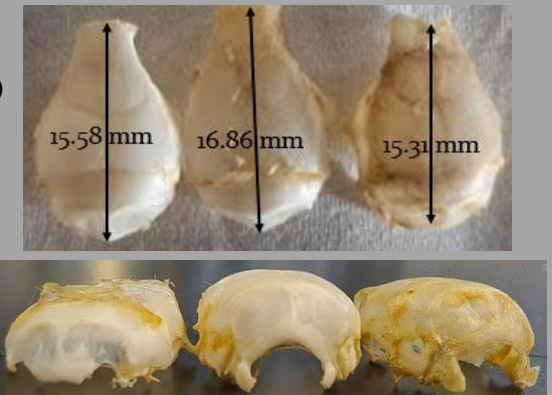


Figure 7: A young mouse (left), middle-aged mouse (middle), and old-aged (right) showing the nonlinear length increase of the skulls with age and the variation in curvature

[4] Junbo Shim et al., *Sci. Rep.*, 2022

[8] M. E. M. Karakatsani, *IEEE Trans Ultrason Ferroelectr Freq Control*, 2017

[5] Elizabeth M. Lillie et al., *ASBMR*, 2015

[9] Matthieu Gerstenmayer et al., *Ultrasound Med Biol*, 2018

[6] Huayue Chen, *Int. J. Endocrinol.*, 2013

[10] Julie C. Crockett et al., *J. Cell Sci.*, 2011

[7] Meaghan A. O'Reilly, *Ultrasound Med Biol*, 2011

[11] Jerel K. Mueller et al., *J. Neural Eng.*, 2017